Association and Aggregation Behavior of Poly (ethylene oxide)-b-Poly (N-isopropylacrylamide) in Aqueous Solution

5 AUTHORS, INCLUDING:

Zichen Li
Peking University

161 PUBLICATIONS   **3,507** CITATIONS

Association and Aggregation Behavior of Poly(ethylene oxide)-*b*-Poly(*N*-isopropylacrylamide) in Aqueous Solution

Jingjing Yan, Wenxi Ji, Erqiang Chen, Zichen Li, and Dehai Liang*

Beijing National Laboratory for Molecular Science and the Key Laboratory of Polymer Chemistry & Physics of Ministry of Education, College of Chemistry & Molecular Engineering, Peking University, Beijing 100871, P. R. China

ABSTRACT: The well-defined block copolymer of poly(ethylene oxide)-*b*-poly(*N*-isopropylacrylamide) (PEO-*b*-PNIPAm) was synthesized by the reversible addition fragmentation transfer (RAFT) polymerization, and its thermo-induced aggregation process in dilute aqueous solution was studied by laser light scattering. At temperatures below the cloud point of PNIPAm, the PEO-*b*-PNIPAm chains were associated together to form large and loose structures, which were in a fast equilibrium with the single chains. The association was weakened with increasing concentration, which was against the common ideas about aggregation. Because of such "abnormal" behavior, PEO-*b*-PNIPAm underwent three stages of transformation during the heating process at 0.1 mg/mL: the disassociation of loose associates at temperatures below 28 °C, the micellization above 42 °C, and the aggregation in between. At each stage, the size and $M_{w,app}$ exhibited distinct features. On the basis of these observations, possible mechanisms of the association and aggregation were also proposed.

Introduction

Thermoresponsive polymers have attracted a great deal of attention in the past few decades due to their potential applications in drug-delivery and as intelligent materials. The developments in this field have been summarized in several excellent reviews.[1,2] Poly(*N*-isopropylacrylamide) (PNIPAm) is one of the most widely studied thermoresponsive polymers. At the temperature below its cloud point, PNIPAm dissolves well in water, while above the cloud point, it will undergo a phase separation because of the breakdown of the hydrogen bonds present at lower temperature.[3–6] Particularly, when the interchain aggregation was avoided,[7–9] a so-called "coil-to-globule" transition can be observed for PNIPAm. The exact definition of LCST of PNIPAm is the critical temperature at the lowest point on the coexistence curve in the PNIPAm/water phase diagram. In many cases, it was the cloud point, instead of the theoretical LCST, that was actually studied. However, sometimes they were used interchangeably in literature. The cloud point of PNIPAm solution was usually considered to be around 32 °C, and it was dependent on many factors, such as molecular weight[10] and end-group.[11]

The thermoresponsive PNIPAm segment also brings interesting properties to the "double-hydrophilic" block and graft copolymers containing it. These polymers will generally form micelles with PNIPAm as the core and the other hydrophilic block as the shell at temperatures above a critical point.[12–16] Such critical micellization temperature (cmt) may be around the cloud point of the PNIPAm or higher, depending on the chemical structure and percentage of the other constituent of the copolymer, concentration, ionic strength, etc. Among all these thermoresponsive copolymers, PNIPAm-*g*-PEO and PEO-*b*-PNIPAm are of particular interest. Tenhu and Virtanen[17] investigated the influence of the number and distribution of the grafted PEO on the thermal properties of PNIPAm-*g*-PEO. Wu and co-workers[18] studied the core–shell nanoparticle formed by PNIPAm-*g*-PEO through the "coil-to-globule" transition, and they found that the final size of the nanoparticle was determined

by the competition between the intrachain and interchain aggregation. Recently, they investigated the folding and unfolding of the individual PNIPAm-*g*-PEO chains during the heating and cooling process.[19]

Compared to the numerous work on graft copolymers, the study on PEO-*b*-PNIPAm is however limited. Tenhu and co-workers[20] prepared a series of PEO-*b*-PNIPAm polymers with the NIPAm/EO ratio ranging from 13 to 244 and studied the micellization process of these polymers in aqueous solution. They found that the aggregate size and structure were dependent on the concentration as well as the constituent of the copolymer. To obtain a narrowly distributed PEO-*b*-PNIPAm block copolymer, Feijen et al.[21] developed a "quasi-living" polymerization technique using the Ce^{4+} redox initiating system. They succeeded in synthesizing PEO-*b*-PNIPAm diblock copolymers as well as PNIPAm-*b*-PEO-*b*-PNIPAm triblock copolymers with relatively low polydispersity. Employing the same technique, Annaka and co-workers[22] synthesized three relatively narrowly distributed block copolymers with different block lengths and investigated the self-assembly of these block copolymers in detail whereby they obtained the binary phase diagram of these block copolymers in solution. Zhang et al.[23] synthesized a narrowly distributed PEO-*b*-PNIPAm by atomic transfer radical polymerization and reported that the aggregate of PEO-*b*-PNIPAm formed at high concentration was much smaller and denser than that formed at low concentration.

It should be noted that most of the published work focused on the micelles formed at temperatures above the cmt, where the collapsed PNIPAm formed the core and the hydrated PEO formed the shell.[24] Few have studied the behavior of PEO-*b*-PNIPAm below cmt. Since water was a good solvent for both PEO and PNIPAm at lower temperature, PEO-*b*-PNIPAm was usually considered to exist as single chains. However, Feijen et al.[21] observed aggregation in the aqueous solution of PEO-*b*-PNIPAm at temperatures below its cloud point. Annaka and co-workers[22] also reported that the formation of disordered micelles started from as low as 17 °C, far below the cmt.

Thus, it would be interesting to explore the aggregates presented in the aqueous solutions of PEO-*b*-PNIPAm at

* Corresponding author. E-mail: dliang@pku.edu.cn. Phone & Fax: 10-86-62756170.

Scheme 1. Synthetic Procedure for PEO$_{44}$−*b*−PNIPAm$_{95}$
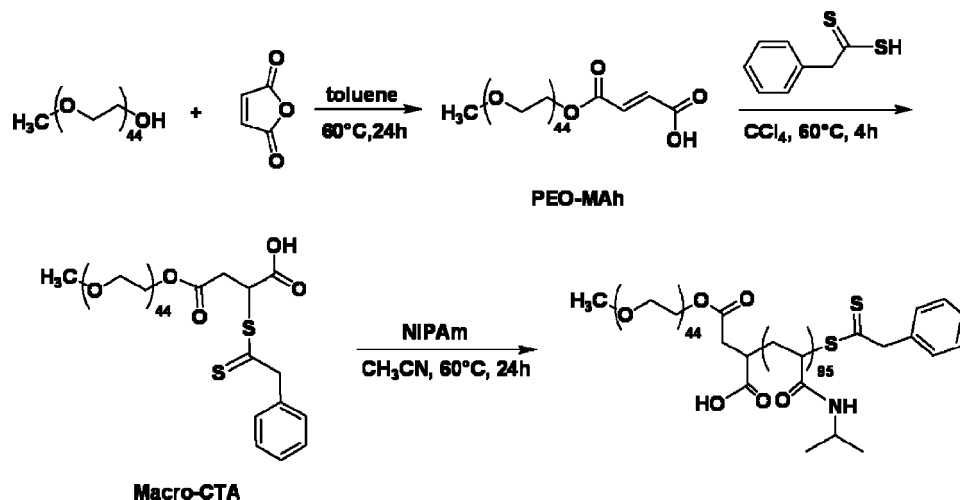
temperatures below cmt and to investigate its effect on the micellization during the heating process. In the present work, we synthesized a narrowly distributed PEO-*b*-PNIPAm by reversible addition fragmentation transfer (RAFT) method and studied its aggregation behavior in dilute solution (0.1 to 1.0 mg/ml) in a wide temperature range by laser light scattering (LLS). We discovered that the PEO-*b*-PNIPAm chains were associated at temperatures below cmt and the degree of association was closely related with concentration. With increasing temperature from 15 to 55 °C, PEO-*b*-PNIPAm at 0.1 mg/mL underwent three stages of transformation: disassociation, aggregation, and micellization. Based on the experimental results, we proposed a possible mechanism for the association of PEO-*b*-PNIPAm at temperatures below its cmt.

Experimental Section

Materials. Poly(ethylene glycol) monomethyl ether (mPEO, $\overline{M}_n \sim 2{,}000, \overline{M}_w/\overline{M}_n \sim 1.10$) was purchased from Fluka (Switzerland). NIPAm obained from Aldrich (USA), was recrystallized twice in a mixture of benzene/hexane (1:1) before use. 2,2-Azobisisobutyronitrile(AIBN) was obtained from Beijing Chemical Reagent Company (Beijing, China) and was purified twice by recrystallization in methanol. Other reagents were purchased from Beijing Chemical Reagent Company and used as received. Milli-Q water (Millipore) with resistance higher than 18 MΩ was used throughout the experiments.

Synthesis of PEO Macro-CTA. Phenyldithioacetic acid was prepared according to the known procedure.[25,26] As shown in Scheme 1, maleic anhydride (MAh, 20 g, 200 mmol) and mPEO (20 g, 10 mmol) was dissolved in 50 mL toluene and allowed to react at 60 °C for 24 h. The resultant mixture was then precipitated in cold diethylether and collected by filtration to obtain PEO−MAh. In the next step, PEO−MAh (10 g, 5 mmol) and phenyldithioacetic acid (approximately 10 g, 60 mmol) were mixed with 80 mL CCl$_4$ and reacted at 60 °C for 4 h. The resulting solution was then precipitated twice in cold diethylether and dried in vacuum to obtain PEO macro-CTA.

Synthesis of PEO-*b*-PNIPAm. As shown in Scheme 1, NIPAm (1.36 g, 12 mmol), PEO macro-CTA (0.24 g, 0.1 mmol), AIBN (1.5 mg, 0.09 mmol) along with acetonitrile (15 mL) were added to a reaction tube. After three freeze–pump–thaw cycles to remove oxygen, the reaction tube was sealed and placed in a thermostatted oil bath at 60 °C for 24 h. The polymerization was then quenched by merging the tube in liquid nitrogen, and PEO-*b*-PNIPAm was recovered by precipitation in cold diethylether followed by filtration and drying in vacuum for 48 h. The yield was about 50%.

Characterization. The molecular weight and the molecular weight distribution of PEO-*b*-PNIPAm were measured by using a gel permeation chromatography (GPC) system, which was equipped with a Waters 2410 refractive index detector, a Waters 515 HPLC pump, and three Waters Styragel columns (HT2, HT3, and HT4). The columns were thermostatted at 35 °C. THF at a flow rate of 1 mL /min was used as the eluent. The molecular weight was calibrated by using the polystyrene standards. GPC results showed that the block copolymer had an average molecular weight M_n of 11 600 and a polydispersity of ca. 1.12.^{1}H NMR spectra was recorded on a Bruker 400M spectrometer at 20 °C by using D$_2$O as the solvent.

Sample Preparation. The stock solution of block copolymer was prepared by directly dissolving the polymer powder in water and allowing it to stay overnight to ensure complete dissolution. The resulting stock solution was then diluted to the desired concentration with proper amount of water. For LLS measurements, the solution was filtered through a 0.22 μm Millipore PVDF filter into a dust-free vial. During the experiment, the sample vial was placed in a brass holder with a precise temperature (±0.01 °C) control. The sample was first cooled to 15 °C and then heated step by step. Measurements were carried out after the sample reached equilibrium.

Light Scattering Measurements. Static light scattering (SLS) and dynamic light scattering (DLS) experiments were conducted on a commercial spectrometer (Brookhaven Inc., Holtsville, NY) equipped with a BI-200SM goniometer and a BI-TurboCorr digital correlator. A solid-state laser polarized at the vertical direction (GXL-III, 100 mW, CNI, Changchun, China) operating at 532 nm was used as the light source. SLS measurements were carried out at scattering angles in the range of 20−120°. The time averaged excess scattered intensity at angle θ, also known as the Rayleigh ratio $R_{vv}(q)$, was related with the weight-averaged molar mass M_w, the Z-averaged root-mean-square radius R_g, the second virial coefficient A_2, and the scattering vector q as

$$\frac{KC}{R_{vv}(q)} \approx \frac{1}{M_w}\left(1 + \frac{1}{3}R_g^2 q^2\right) + 2A_2 C \tag{1}$$

where $K = 4\pi n^2 (dn/dc)^2/(N_A \lambda_0^4)$ and $q = (4\pi n/\lambda)\sin(\theta/2)$, with N_A, n, (dn/dc), and λ_0 being the Avogadro constant, the refractive index of the solvent, the specific refractive index increment of the solution, and the wavelength of light in vacuum, respectively.

The (dn/dc) value of the PEO-*b*-PNIPAm copolymer can be estimated by the following equation,

$$dn/dc = W_{PEO}(dn/dc)_{PEO} + W_{PNIPAm}(dn/dc)_{PNIPAm} \tag{2}$$

where W denotes the weight percentage of a certain block. The dn/dc values of PEO and PNIPAm were obtained from literature.[18,23]

For dynamic scattering, the intensity–intensity time autocorrelation function $G^{(2)}(t,\theta)$ was measured in the self-beating mode. It
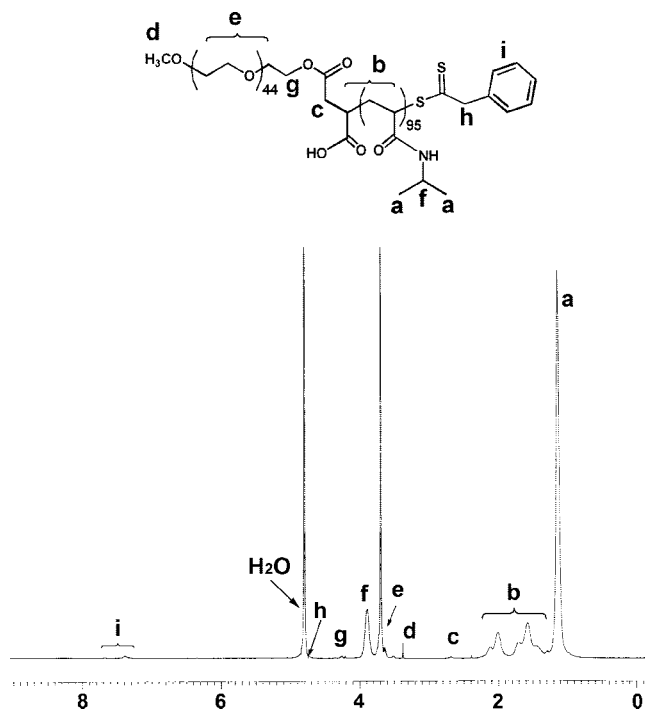
Figure 1. ^{1}H NMR spectrum of PEO$_{44}$-b-PNIPAm$_{95}$ in D$_2$O at 20 °C.

Figure 2. CONTIN analysis of PEO$_{44}$-b-PNIPAm$_{95}$ at different concentrations at 15 °C, $\theta = 30°$. The spectra have been normalized by the peak height at 3 nm for better comparison.

Figure 3. $KC/R(\theta)$ *vs* q^2 plot of aqueous solution of PEO$_{44}$-b-PNIPAm$_{95}$ at different concentrations (0.1 ∼ 1.0 mg/mL) at 15 °C. The inset shows the concentration dependence of the apparent molecular weight of the associate.

is related with the normalized first order electric field time correlation function $g^{(1)}(t,\theta)$ as

$$G^{(2)}(t,\theta) = \langle I(0,\theta)I(t,\theta) \rangle = A[1 + \beta |g^{(1)}(t,\theta)|^2] \quad (3)$$

The line width distribution $G(\Gamma)$ was analyzed with a Laplace inversion program, CONTIN, based on the following relation,

$$g^{(1)}(t,\theta) = \langle E(0,\theta)E^*(t,\theta) \rangle = \int_0^\infty G(\Gamma)e^{-\Gamma t}d\Gamma \quad (4)$$

Based on the $\bar{\Gamma}$ of each peak given by the CONTIN program, the diffusion coefficient D can be calculated according to $D = \bar{\Gamma}/q^2$. For a translational diffusion, the hydrodynamic radius R_h can be calculated using the Stokes–Einstein equation:

$$R_h = \frac{k_B T}{6\pi\eta D} \quad (5)$$

Results and Discussion

Figure 1 shows the ^{1}H NMR spectrum of PEO-b-PNIPAm in D$_2$O. The protons in the polymer have been indicated in the figure. The chemical composition of PEO-b-PNIPAm was determined from the ratio of the peak integral of the $-$OCH$_2$CH$_2-$ protons of PEO and the *N*-methyl protons of NIPAm units. It was determined that the repeating units of PEO and PNIPAm were 44 and 95, respectively.

Figure 2 shows the DLS results of PEO-b-PNIPAm in aqueous solution at concentrations ranging from 1.0×10^{-4} to 1.0×10^{-3} g/mL at 15 °C. A characteristic bimodal distribution, indicating the occurrence of the aggregation, was observed at all the studied concentrations. The $R_{h,app}$ value of the smaller component was ∼3 nm and remained constant with changing concentration. Considering the fact that the M_w of PEO-b-PNIPAm was 12 000 Da, we attributed the smaller component to the single polymer chain. Therefore, the larger component was corresponded to the aggregate formed by PEO-b-PNIPAm. Figure 2 also indicated that the $R_{h,app}$ value of the aggregate was decreased from about 55 nm at 0.1 mg/mL to about 20 nm at 1.0 mg/mL. Moreover, the area ratio of the larger component also sharply decreased with increasing concentration. The static light scattering experiments provided consistent results. Figure 3 shows the corresponding $KC/R(\theta)$ *vs* q^2 plots of the PEO-b-

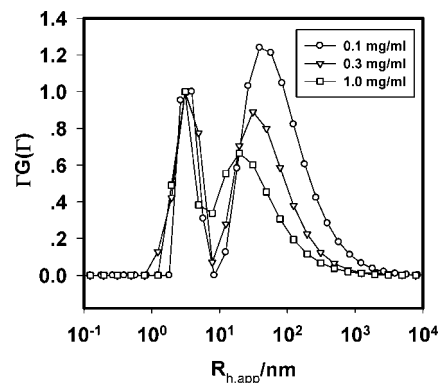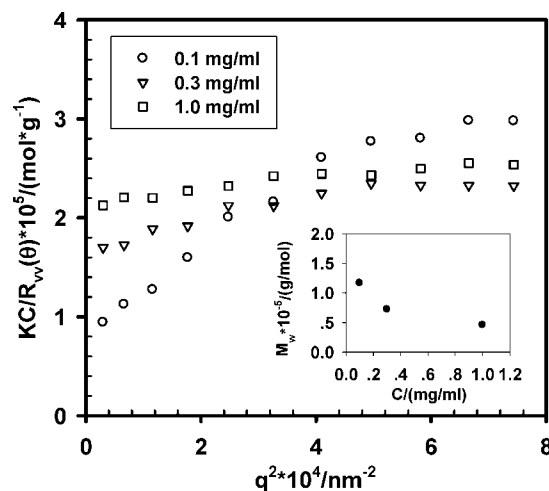PNIPAm in aqueous solution at 15 °C. Because of the presence of aggregates, a downward curve at lower scattering angle was obtained at all the studied concentrations.[27] In such cases, R_g and M_w of the aggregate can be estimated from the extrapolation of the lower q values portion of $KC/R(\theta)$ vs q^2 plot.[28] The resulting apparent molecular weight was plotted in the inset in Figure 3. Clearly, the $M_{w,app}$ decreased with increasing concentration. Similar to that of $R_{h\,app}$, the $R_{g,app}$ value sharply decreased from 119 nm at 0.1 mg/mL to 35 nm on increasing the concentration to 1.0 mg/mL.

Water being a good solvent for both PEO and PNIPAm, PEO-b-PNIPAm was usually considered to exist as single chains in aqueous solution at temperatures below the cmt, and it would form micelles with PNIPAm being the core and PEO being the corona on increasing the temperature to above the cmt. In contrast, our results clearly show the existence of an "abnormal aggregate" formed under good solvent conditions. A possible explanation could be the end-group effect. It is known that the hydrophobic end group could decrease the solubility and induce the aggregation of a hydrophilic polymer, especially when the overall molecular weight is relatively low. This phenomenon has been found in a number of homopolymer systems such as PNIPAm[11] and poly(hydroxyethyl acrylamide).[29] For example, alkyl-terminated PNIPAms formed a hydrophobic core of alkyl chain ends as long as the alkyl end group was large enough.[30–34] However, it should be noted that the "aggregation" in our case became weaker with increasing concentration. If the aggregate
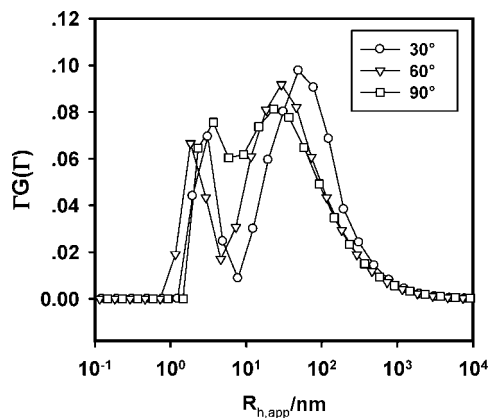
Figure 4. CONTIN analysis of PEO$_{44}$-*b*-PNIPAm$_{95}$ at 0.1 mg/mL at 15 °C, $\theta = 30°$.
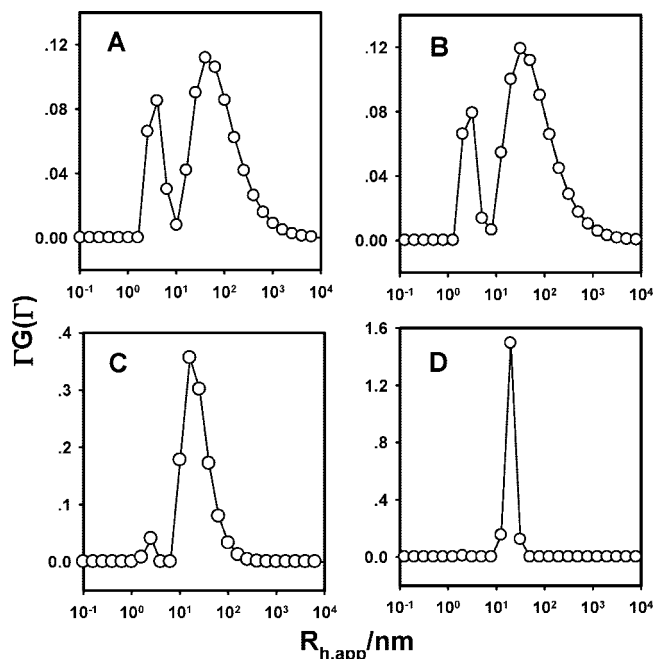

Figure 5. R_h distributions of PEO$_{44}$-*b*-PNIPAm$_{95}$ at 0.1 mg/mL at selected temperatures of (A) 25 °C, (B) 34 °C, (C) 44 °C, and (D) 55 °C; $\theta = 30°$.

Figure 6. Representative $KC/R(\theta)$ *vs* q^2 plots of PEO$_{44}$-*b*-PNIPAm$_{95}$ at 0.1 mg/mL at different temperatures.

Figure 7. Temperature dependence of the apparent hydrodynamic radius $R_{h,app}$ and the apparent radius of gyration $R_{g,app}$ of the associate/aggregate formed in the aqueous solution of PEO$_{44}$-*b*-PNIPAm$_{95}$ (0.1 mg/mL) during a heating process. The inset shows the corresponding changes in $R_{g,app}/R_{h,app}$ ratio.

was simply caused by the end groups, such an "abnormal" concentration dependence of the aggregation behavior could not be explained satisfactorily. Besides, on detaching the dithiobenzoate end groups, no prominent effect on the aggregation behavior was observed (see the Supporting Information). Therefore, the origin and property of the "aggregate", as well as its effect on the temperature induced micellization, all remain very interesting questions.

In order to gain some insight into the nature of the aggregate, we focused our further investigations on the 0.1 mg/mL sample. Figure 4 compares the CONTIN results of PEO-*b*-PNIPAm measured at different angles at 15 °C. An $R_{h,app}$ value of 77 nm was obtained for the aggregate after the angular extrapolation of $D = \bar{\Gamma} q^2$ and the application of the Stocks–Einstein equation. Together with the $R_{g,app}$ value (119 nm) derived from Figure 3, an $R_{g,app}/R_{h,app}$ ratio of 1.5 was obtained. It is well established in literature that the R_g/R_h was a useful parameter to evaluate the conformation of aggregate. Generally speaking, a larger ratio indicates a loose or more extended conformation. Typically, random coils and collapsed globules exhibit R_g/R_h ratios of 1.5 and 0.776, respectively. A core–shelled micelle with a higher density in its center may have an even lower value.[18,35] The
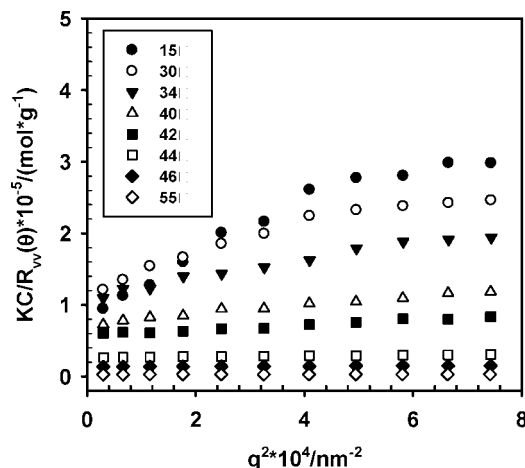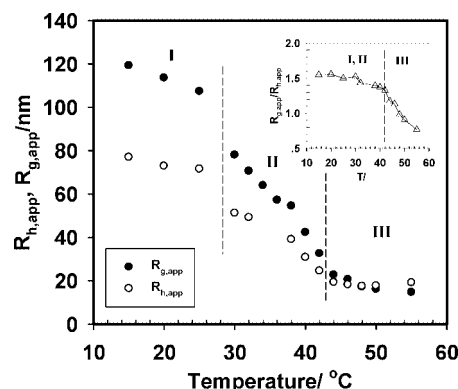
$R_{g,app}/R_{h,app}$ ratio suggested that the abnormal aggregates formed by PEO-*b*-PNIPAm were in a loose conformation. In addition, the $M_{w,app}$ of the aggregate, shown in the inset in Figure 3, was ~1.2×10^5 g/mol, about 10 times higher than that of the single polymer chain ($M_{n,NMR} = 1.2 \times 10^4$ g/mol). Such a low molecular weight or aggregation number, together with the large size, also confirmed that the aggregate formed by PEO-*b*-PNIPAm adopted a loose conformation in aqueous solution at 15 °C. Similar aggregates have also been observed for PEO-*b*-poly(methyl methacrylate) in several nonselective solvents, such as acetone, chloroform, and thetrahydrofuran.[36] The authors attribute them to some types of fluctuating structures.

It has been reported that PEO-*b*-PNIPAm formed core–shell micelle at temperatures above its cmt.[21–24] To figure out the relationship between the loose aggregate and the micelle, we monitored the behavior of PEO-*b*-PNIPAm at 0.1 mg/mL during the heating process by using both DLS and SLS. Figure 5 shows the DLS results at varying temperatures. On increasing the temperature to 25 °C, a bimodal distribution very similar to that at 15 °C was obtained (Figure 5A). When the temperature increased to 34 °C, which was higher than the cloud point of PNIPAm, only slight changes in size or size distribution could be observed (Figure 5B). However, a significant transition occurred at 44 °C, where the size distribution of the aggregate was narrowed down and the ratio of the unimer was sharply decreased (Figure 5C). On increasing the temperature further to 55 °C, only one narrowly distributed component with $R_{h,app}$ of about 20 nm remained in the system (Figure 5D), indicating
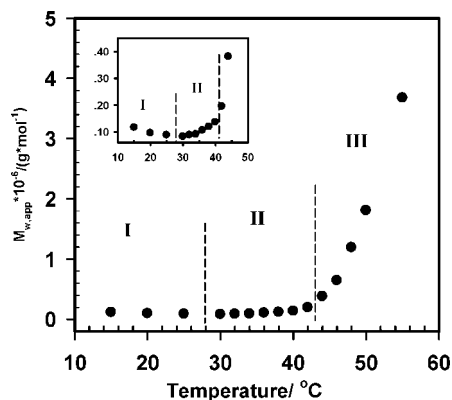
Figure 8. Temperature dependence of the average apparent molecular weight ($M_{w,app}$) of PEO$_{44}$-*b*-PNIPAm$_{95}$ at 0.1 mg/mL. The inset magnifies the changes in $M_{w,app}$ at stages I and II.

the formation of micelles with PEO as the shell and PNIPAm as the core.[24]

The SLS experiments were also carried out during the heating process. Figure 6 shows the $KC/R(\theta)$ vs q^2 curves at selected temperatures. Similar to the $KC/R(\theta)$ vs q^2 plot at 15 °C, all the $KC/R(\theta)$ vs q^2 plots at temperatures below 42 °C were trending downward at lower scattering angles, implying the coexistence of the aggregates and the unimers. At temperatures above 42 °C, $KC/R(\theta)$ exhibited a linear relationship with q^2, and the angular dependence was also reduced with increasing temperature. Again, by using the extrapolation method indicated in Figure 3, we calculated the $R_{g,app}$ and the $M_{w,app}$ values at different temperatures for further evaluation.

Figure 7 compares the $R_{g,app}$ and $R_{h,app}$ values at different temperatures. Clearly, both $R_{g,app}$ and $R_{h,app}$ were decreased with increasing temperature, but with different speed, basing on which the plot in Figure 7 could be divided into three stages. At temperature below 28 °C (stage I), the value of $R_{g,app}$ was larger than that of the $R_{h,app}$, and both of them were slowly decreased with increasing temperature. The sharp decrease in size was occurred in stage II, at temperatures ranging from 28 to 42 °C. The difference between $R_{g,app}$ and $R_{h,app}$ also gradually reduced in stage II. The value of $R_{h,app}$ surpassed that of $R_{g,app}$ at temperatures above 48 °C in stage III. Another feature in stage III was that the changes in size were not prominent. To view the conformational change of the aggregate more clearly, the temperature dependence of the $R_{g,app}/R_{h,app}$ ratio was also plotted in the inset in Figure 7. In stages I and II, the $R_{g,app}/R_{h,app}$ ratio slowly decreased from 1.54 at 15 °C to about 1.32 at 42 °C. While at temperatures above 42 °C (stage III), the ratio dramatically decreased and finally it reached 0.78 at 55 °C.
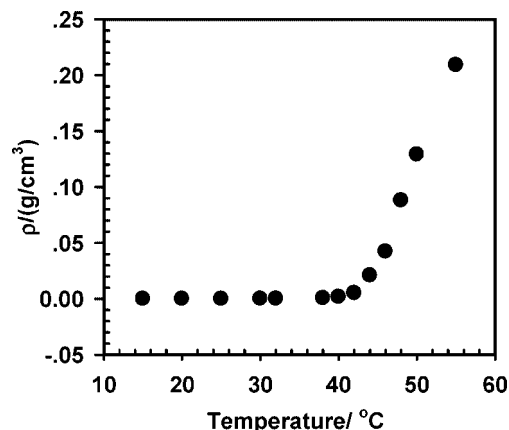

Figure 9. Changes in the apparent average chain density of the associate/aggregate of PEO$_{44}$-*b*-PNIPAm$_{95}$ at 0.1 mg/mL during a heating process.

Figure 8 shows the changes in $M_{w,app}$ with increasing temperature, which is also correspondingly divided into the same three temperature stages as in Figure 7. For a better view, stages I and II were magnified in the inset in Figure 8. In stage I, $M_{w,app}$ slowly decreased from 1.2×10^5 g/mol at 15 °C to 8.0×10^4 g/mol at 25 °C, which corresponds to a decrease in the aggregation number from 10 to 7. After the $M_{w,app}$ reached the minimum at 25 °C or so, the system entered the stage II, wherein the $M_{w,app}$ started to increase, indicating the occurrence of heavier aggregation. However, the aggregation was only limited to a few more chains (<16), because the $M_{w,app}$ at 42 °C was less than 1.9×10^5 g/mol. The sharp increase in $M_{w,app}$ was observed in stage III, where the $M_{w,app}$ increased by nearly 90 times from 44 to 55 °C. It is interesting to note that no plateau of $M_{w,app}$ was observed in the temperature range of our experiment. It was different from the findings on PNIPAm-*g*-PEO by Qiu et al.,[35] where PNIPAm-*g*-PEO formed stable mesoglobules at a certain temperature above which the inter-chain aggregation was diminished.

Combining the results in Figures 7 and 8, we can estimate the apparent chain density of the aggregates according to the following equation:[35]

$$\rho = \frac{3M_{w,app}}{4N_A R_h^3} \qquad (6)$$

As shown in Figure 9, the chain density was extremely low at temperatures below 42 °C, indicating that the aggregate contained a large amount of solvent molecules or was in a loose conformation. A sharp increase in chain density was observed at temperatures above 42 °C, i.e., in stage III, suggesting that the solvent molecules were "squeezed" out from the aggregates.

Scheme 2. Illustration of the Three Distinct Stages of the PEO$_{44}$-*b*-PNIPAm$_{95}$ Chains at 0.1 mg/mL during a Heating Process: (A) Associates at Temperatures Below 28 °C, (B) Loose Aggregates Formed between 28 and 42 °C, and (C) Micelles at above 42 °C
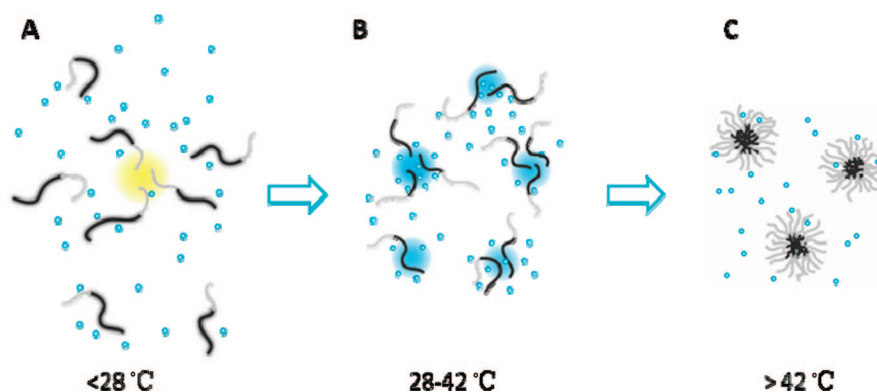
On the basis of the above results, together with the findings about PNIPAm and PEO-*b*-PNIPAm in the literature, we were able to rationally explain the aggregation behavior of PEO-*b*-PNIPAm during the heating process. As schematically shown in Scheme 2, PEO-*b*-PNIPAm underwent three stages of transformation, namely disassociation, aggregation, and micellization with increasing temperature from 15 to 55 °C. At temperatures below the cloud point of PNIPAm (stage I), water was a good solvent for both PEO and PNIPAm. PEO-*b*-PNIPAm was in a random coil conformation. However, due to the incompatibility between PNIPAm and PEO (χ_{AB}), some of the PEO-*b*-PNIPAm chains associated together to form the structure containing PEO-rich and PNIPAm-rich domains (panel A). Since the entropy favored the uniform mixing of PEO and PNIPAm, it was against the formation of such structures. Note that such a structure built a fast equilibrium with the single chains, and its number was far less than that of the single chains. In the case where the PEO blocks or the PNIPAm blocks are difficult to form the domains, the associated structure will be destroyed. With increasing concentration, the chances for the same number of PEO blocks to "meet" in a given volume for a given time period (prerequisite to form the domain) decreased because of the interference of PNIPAm blocks and vice versa, which led to a decrease in domain size and a shift of the equilibrium to the single chains (Figures 2 and 3). An increase in temperature enhanced the hydrophobicity of PNIPAm block and thus changed the χ_{AB} value. Meanwhile, it also increased the contribution from entropy. Both of these caused the structures in panel A to gradually disassociate (stage I in Figures 7 and 8).

On increasing the temperature further, water slowly became a slightly selective solvent for PNIPAm blocks (stage II) and thus PNIPAm blocks started to shrink and tended to aggregate. The critical temperature at which water became selective could be lower than the cloud point of PNIPAm[22]. Also, because of the solubility of PEO, free single chains still widely existed in this stage and no sharp transition from coil to globule was observed. Only relatively loose aggregates, containing a PNIPAm rich domain, were formed at temperatures above the cloud point of PNIPAm (panel B). Such aggregates were believed to act as precursors for micelle formation. On further increasing the temperature to enhance the shrinking and aggregation force from PNIPAm, a sharp reduction in size (Figure 7) and an increase in $M_{w,app}$ (Figure 8) were observed. At temperatures above 42 °C (stage III), PNIPAm blocks collapsed and the solubility force of PEO was relatively not important any more. The primary micelles, with PNIPAm being the core and PEO being the corona, were formed (panel C), and the number of unimers quickly diminished. A further increase in temperature at this stage led to the condensation and fusion of the micelles, which is demonstrated by the sharp increase in $M_{w,app}$ (Figure 8) as well as chain density (Figure 9).

Conclusion

We have prepared a narrowly distributed block copolymer of PEO$_{44}$-*b*-PNIPAm$_{95}$ using RAFT technique and studied the thermoinduced aggregation process of the well-defined PEO-*b*-PNIPAm diblock copolymer in dilute aqueous solution by dynamic and static light scattering techniques. We found that the block copolymer formed large and loose structures at the temperature stage where water was a good solvent for both of the blocks. Such structures were in a fast equilibrium with the free copolymer chains. The size and proportion of this loose structure decreased with increasing concentration. Based on the observations, we attributed the driving force of the structure to the incompatibility between the two blocks. Because of the loose structure at lower temperature, PEO-*b*-PNIPAm at 0.1 mg/mL underwent three stages of transformation, namely disassociation, aggregation, and micellization in sequence during the heating process.

Supporting Information Available: Detachment of end group and LLS study on aggregation. This information is available free of charge via the Internet at http://pubs.acs.org.

References and Notes

(1) Gil, E. S.; Hudson, S. A. *Prog. Polym. Sci.* **2004**, *29* (12), 1173–1222.
(2) Jeong, B.; Gutowska, A. *Trends in Biotechnology* **2002**, *20* (7), 305–311.
(3) Kubota, K.; Fujishige, S.; Ando, I. *J. Phys. Chem.* **1990**, *94* (12), 5154–5158.
(4) Okada, Y.; Tanaka, F. *Macromolecules* **2005**, *38* (10), 4465–4471.
(5) Ono, Y.; Shikata, T. *J. Am. Chem. Soc.* **2006**, *128* (31), 10030–10031.
(6) Schild, H. G. *Prog. Polym. Sci.* **1992**, *17* (2), 163–249.
(7) Wang, X. H.; Qiu, X. P.; Wu, C. *Macromolecules* **1998**, *31* (9), 2972–2976.
(8) Wu, C.; Zhou, S. Q. *Macromolecules* **1995**, *28* (24), 8381–8387.
(9) Wu, C.; Zhou, S. Q. *Macromolecules* **1995**, *28* (15), 5388–5390.
(10) Xia, Y.; Yin, X. C.; Burke, N. A. D.; Stover, H. D. H. *Macromolecules* **2005**, *38* (14), 5937–5943.
(11) Xia, Y.; Burke, N. A. D.; Stover, H. D. H. *Macromolecules* **2006**, *39* (6), 2275–2283.
(12) Xu, Y. L.; Shi, L. Q.; Ma, R. J.; Zhang, W. Q.; An, Y. L.; Zhu, X. X. *Polymer* **2007**, *48* (6), 1711–1717.
(13) Ge, Z. S.; Luo, S. Z.; Liu, S. Y. *J.Polym. Sci., Part A: Polym. Chem.* **2006**, *44* (4), 1357–1371.
(14) Zareie, M. H.; Dincer, S.; Piskin, E. *J. Colloid Interface Sci.* **2002**, *251* (2), 424–428.
(15) Konak, C.; Reschel, T.; Oupicky, D.; Ulbrich, K. *Langmuir* **2002**, *18* (21), 8217–8222.
(16) Kim, I. S.; Jeong, Y. I.; Cho, C. S.; Kim, S. H. *Int. J. Pharm.* **2000**, *211* (1–2), 1–8.
(17) Virtanen, J.; Tenhu, H. *Macromolecules* **2000**, *33* (16), 5970–5975.
(18) Qiu, X. P.; Wu, C. *Macromolecules* **1997**, *30* (25), 7921–7926.
(19) Chen, H. W.; Li, J. F.; Ding, Y. W.; Zhang, G. Z.; Zhang, Q. J.; Wu, C. *Macromolecules* **2005**, *38* (10), 4403–4408.
(20) Virtanen, J.; Holappa, S.; Lemmetyinen, H.; Tenhu, H. *Macromolecules* **2002**, *35* (12), 4763–4769.
(21) Topp, M. D. C.; Dijkstra, P. J.; Talsma, H.; Feijen, J. *Macromolecules* **1997**, *30* (26), 8518–8520.
(22) Motokawa, R.; Morishita, K.; Koizumi, S.; Nakahira, T.; Annaka, M. *Macromolecules* **2005**, *38* (13), 5748–5760.
(23) Zhang, W. Q.; Shi, L. Q.; Wu, K.; An, Y. G. *Macromolecules* **2005**, *38* (13), 5743–5747.
(24) Maeda, Y.; Taniguchi, N.; Ikeda, I. *Macromol. Rapid Commun.* **2001**, *22* (17), 1390–1393.
(25) Barner-Kowollik, C.; Quinn, J. F.; Nguyen, U. L.; Heuts, J. P. A.; Davis, T. P. *Macromolecules* **2001**, *34* (22), 7849–7857.
(26) Hong, C. Y.; You, Y. Z.; Pan, C. Y. *J.Polym. Sci., Part A: Polym. Chem.* **2004**, *42* (19), 4873–4881.
(27) Evans, J. M. Manipulation of Light Scattering Data. In *Light Scattering from Polymer Solution*, Huglin, M. B., Ed. Acadamic Press: New York, 1972; p 132.
(28) Zuo, J. *Application of laser Light Scattering in Polymer Science*. 1st ed.; Henan Science & Technology Press: Tianjin, 1995.
(29) Weaver, J. V. M.; Bannister, I.; Robinson, K. L.; Bories-Azeau, X.; Armes, S. P.; Smallridge, M.; McKenna, P. *Macromolecules* **2004**, *37* (7), 2395–2403.
(30) Ringsdorf, H.; Venzmer, J.; Winnik, F. M. *Macromolecules* **1991**, *24* (7), 1678–1686.
(31) Chung, J. E.; Yokoyama, M.; Suzuki, K.; Aoyagi, T.; Sakurai, Y.; Okano, T. *Colloids Surf., B* **1997**, *9* (1–2), 37–48.
(32) Chung, J. E.; Yokoyama, M.; Aoyagi, T.; Sakurai, Y.; Okano, T. *J. Controlled Release* **1998**, *53* (1–3), 119–130.
(33) Kujawa, P.; Winnik, F. M. *Macromolecules* **2001**, *34* (12), 4130–4135.
(34) Kujawa, P.; Segui, F.; Shaban, S.; Diab, C.; Okada, Y.; Tanaka, F.; Winnik, F. M. *Macromolecules* **2006**, *39* (1), 341–348.
(35) Chen, H. W.; Zhang, Q. J.; Li, J. F.; Ding, Y. W.; Zhang, G. Z.; Wu, C. *Macromolecules* **2005**, *38* (19), 8045–8050.
(36) Edelmann, K.; Janich, M.; Hoinkis, E.; Pyckhout-Hintzen, W.; Horing, S. *Macromol. Chem. Phys.* **2001**, *202* (9), 1638–1644.